



Dear Readers,

With this issue, I am leaving the Editorship of THE MESSENGER, a task which I valued and enjoyed. The Editorship now passes to my ESO colleague Peter Shaver.

MARIE-HÉLÈNE DEMOULIN

NAOS+CONICA at YEPUN: First VLT Adaptive Optics System Sees First Light

W. BRANDNER, G. ROUSSET, R. LENZEN, N. HUBIN, F. LACOMBE, R. HOFMANN,
A. MOORWOOD, A.-M. LAGRANGE, E. GENDRON, M. HARTUNG, P. PUGET, N. AGEORGES,
P. BIEREICHEL, H. BOUY, J. CHARTON, G. DUMONT, T. FUSCO, Y. JUNG, M. LEHNERT,
J.-L. LIZON, G. MONNET, D. MOUILLET, C. MOUTOU, D. RABAUD, C. RÖHRLE, S. SKOLE,
J. SPYROMILIO, C. STORZ, L. TACCONI-GARMAN, G. ZINS

1. Introduction

NAOS+CONICA (hereafter NACO) saw first light on November 25, 2001, at VLT UT4 (YEPUN). NACO partially compensates the effects of atmospheric turbulence (seeing) and provides diffraction-limited resolution for observing wavelengths from 1 to 5 μm , resulting in a gain in spatial resolution by a factor of 5 to 15 (diffraction limit of an 8-m-class telescope in K-band corresponds to 60 mas). This article gives an overview of the main characteristics and science drivers of NACO and briefly summarises the first results obtained during commissioning. Prospective users of NACO are kindly asked to cite [7] and [13] as a general reference to NACO in their scientific papers.

2. History

Adaptive Optics (AO) has a long history at ESO, stretching back to the early operations of COME-ON, COME-ON+,

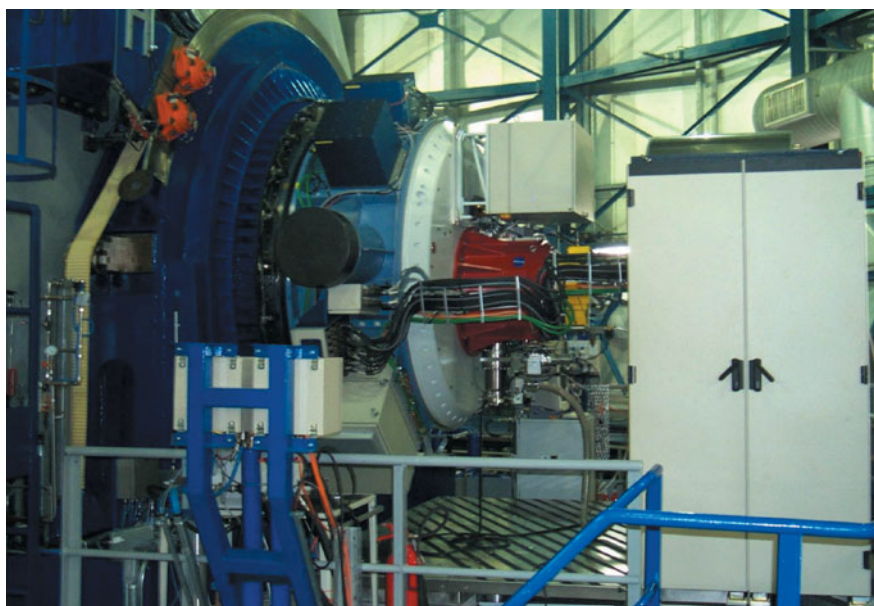


Figure 1: NAOS (light blue) and CONICA (red) attached to the Nasmyth B adapter of Yepun/UT4.



Figure 2: The triple system *T Tauri*. Shown on the left is an open-loop image (obtained through a narrow-band filter at $2.16\ \mu\text{m}$ with an exposure time of 0.4 sec). Only the $0.7''$ binary *T Tauri* North and South is resolved, while the close binary *T Tauri* South itself remains unresolved. The image in the middle was obtained with the same instrumental set-up, but with the AO loop closed. The $0.1''$ binary *T Tauri* South is now nicely resolved. The image to the right finally shows a 2D long-slit K-band spectrum of both components of *T Tauri* South.

and finally ADONIS at the ESO 3.6-m telescope on La Silla (see [1], [6]). Based on this experience, an early decision was made to equip the VLT coude foci with AO systems ([9]).

CONICA (the COude Near-Infrared CAmera), a 1 to $5\ \mu\text{m}$ infrared camera for diffraction-limited imaging and spectroscopy, was proposed by a consortium of the Max-Planck-Institut für Astronomie, Max-Planck-Institut für Extraterrestrische Physik, and the Osservatorio Astronomico di Torino in response to an ESO Call for Proposals. It was selected in 1991 as one of the first-generation VLT instruments. Subsequent re-organisations in the VLT schedule led to the (temporary) cancellation of the AO equipped coude foci and the loss of the Osservatorio Astronomico di Torino to the CONICA project. In 1994 studies for implementing AO at the VLT Nasmyth foci were initiated ([5]) and, in parallel, an effort started to re-design CONICA and transform it into an instrument for a Nasmyth focus. In 1997, a consortium consisting of Office National d'Etudes et Recherches Aérospatiales (ONERA), Observatoire de Paris and Laboratoire d'Astrophysique de l'Observatoire de Grenoble was awarded a contract to develop and build the Nasmyth AO System (NAOS) for the VLT.

After a period of integrated testing at the CNRS facilities in Bellevue, near Paris, NACO was shipped to Paranal in October 2001 and achieved its first light at UT4 at the end of November 2001.

Figure 1 shows NACO mounted at Nasmyth B of UT4. More detailed information can be found at <http://www.eso.org/instruments/naco>

3. Instrumental Characteristics and Science Drivers

3.1 NAOS

NAOS ([13]) is a state-of-the-art AO system optimised for operation at the VLT telescopes, and designed to provide a Strehl ratio (SR) of $\geq 70\%$ in the K band when wavefront sensing on a bright natural reference source under average atmospheric conditions on Paranal (yet not compromising its compensation capabilities on very faint sources – $V \geq 16$ mag and $K \geq 12$ mag). Active optical elements of NAOS include a tip-tilt plane mirror and a deformable mirror (DM) with 185 actuators. NAOS is equipped with two Shack-Hartmann type wavefront sensors (WFS) for wavefront sensing in the optical (450 to 950 nm) and in the near-infrared (0.8 to $2.5\ \mu\text{m}$).

Both the visual and infrared wavefront sensor can be operated either in 14×14 array configuration with 144 active subapertures (in the pupil) or in 7×7 array configuration with 36 active subapertures. A range in fields of view per subaperture, temporal sampling frequencies, and pixel scales (binning) of the WFS are available in order to provide optimal performance over a very wide range of observing conditions and reference source characteristics. Dichroics split the light between the wavefront sensing channel (NAOS IR or vis WFS) and the science channel (CONICA). Reference sources for wavefront sensing can be selected at angular separations of up to $60''$ from the on-axis science target. Guiding on reference sources with a relative motion is of course possible, and the differential atmospheric refraction be-

tween NAOS and CONICA is also taken into account. Last but not least, NAOS can handle VLT M2 beam chopping in order to provide CONICA with the best observing conditions in the thermal infrared.

The NAOS Real Time Computer (RTC) constitutes a highly optimised symbiosis of hardware and software elements ([12]), and is capable of controlling the Adaptive Optics at frequencies up to 444 Hz. It continuously monitors the turbulence and the optimisation of the correction, taking into account the detected brightness of the reference source. It has been designed to easily facilitate the upgrade to a Laser Guide Star (see [2] for more details on the VLT Laser Guide Star facility).

Initial testing indicates that NAOS is delivering full correction (on-axis Strehl ratio of up to 50% in K-band for average atmospheric conditions on Paranal) for a reference source with $V = 12$ mag. Still higher Strehl ratios might be achievable after various instrument parameters have been fine tuned. The adaptive optics loop has been closed on point sources as faint as $V = 17.5$ mag (vis. WFS) and $K = 12$ mag (IR WFS).

3.2 CONICA

CONICA ([7]) operates with the $f/15$ beam, which is passed through NAOS from the Nasmyth B focus of UT4. CONICA is equipped with a 1024×1024 pixel ALADDIN2 InSb detector (pixel size $27 \times 27\ \mu\text{m}$). The ALADDIN2 detector is sensitive to radiation between 0.9 and $5\ \mu\text{m}$, and is operated at a temperature of 27K. Instrumental background is below $1\ \text{e}^-/\text{s}$. CONICA uses

Table 1: List of available Cameras with f-ratios, scales, magnification, field of view, wavelength range.

Camera	f-ratio	Scale [mas/pixel]	Magnification	FOV [arcsec]	Spectral range
C50S	52.7	13.25	3.50	13 × 13	1–2.5 μm
C25S	25.8	27.03	1.72	27 × 27	1–2.5 μm
C12S	12.8	54.3	0.85	54 × 54	1–2.5 μm
C06S	6.36	109.3	0.425	73 \emptyset	1–2.5 μm
C25L	25.7	27.12	1.71	27 × 27	2.5–5.0 μm
C12L	12.7	54.7	0.85	54 × 54	2.5–5.0 μm
C06L	6.33	109.9	0.42	73 \emptyset	2.5–5.0 μm

the ESO-developed IRACE readout electronics and acquisition software ([10]). The read-out noise is $40e^-$ for double correlated read-out (ReadReset Read), and can be reduced to $\leq 10e^-$ for longer exposures by using Fowler sampling (FowlerNSamp). Sustainable data rates can be as high as 2 MByte/s (i.e., one full frame saved to disk every two seconds), and exposure times can be as short as 0.2 sec for full frame read-out (or even shorter for windowed read-out) and for short sequences of up to 8 exposures or by using the NDIT > 1 option (frames averaged by IRACE).

CONICA houses seven cameras, which provide Nyquist sampling for the corresponding bands between 1 and 5 μm (see Table 1). Four of the cameras are optimised for observations between 1 and 2.5 μm with pixel scales of 13.25 mas/pixel (C50S camera), 27.03 mas/pixel (C25S camera), 54.1 mas/pixel (C12S camera) and 107 mas/pixel (C06S), and three of the cameras are optimised for observations between 2 and 5 μm (C25L, C12L, C06L with corresponding pixel scales). The field of view for individual cameras ranges from 13" × 13" (C50S) to a circular aperture of 73" diameter (C06S and C06L).

A large variety of optical analysing elements can be rotated into the CONICA beam. For broad- and narrow-band imaging one can select among 34 different filters. Polarimetric observations are supported both by two Wollaston prisms (split approx. 3.4" in K-band for dual imaging observations) and four wiregrids ("wide field"). For spectroscopy one can choose between four grisms (R = 500 to 2000, with various orders covering the range from 1 to 5 μm) and a cryogenic Fabry-Perot with a resolution of around 1000. Coronagraphy is supported by a Lyot-type coronagraph with mask diameters ranging from 0.7" to 1.4".

3.3 Science Drivers

The science drivers for NACO were early on defined by the CONICA Instrument Science Team chaired by Marie-Hélène Ulrich. The working

group identified both Galactic and extragalactic science drivers:

Galactic astronomy

- Outflows and disks of young stellar objects
- Search for low-mass/substellar companions of nearby stars
- Structure of young embedded objects
- Ionisation fronts in HII regions
- Galactic centre
- Close companions and circumstellar material around T Tauri stars
- Structure of Red Giant envelopes

Extragalactic astronomy

- Quasars and host galaxies
- Emission line imaging of super-luminous IRAS galaxies
- Search for Black Holes in centres of galaxies
- Resolved images of radio jets and hot spots
- Obscured quasars
- The cosmic distance scale

In addition, NACO will facilitate high spatial resolution studies of Solar system objects and astronomical targets in the solar neighbourhood.

4. Observing with NACO

4.1 Preparation of Observations

All AO observations depend on the availability of a reference source suitable for wavefront sensing. Thus a crucial part in the preparation of observations with NACO is to check for such a reference source in the proximity to the science target. The minimal requirement for partial correction by NACO will be a point source with $V < 17.5$ mag or $K < 12$ mag within 60" of the science target. Due to the presence of angular anisoplanatism (see [14]), the best AO correction is achieved in the on-axis case (science target identical with reference source). Online versions of the Guide Star Catalog 2 and the 2MASS point source catalog aid the prospective user of NACO in the search for suitable reference sources (follow links on the main NACO web

page <http://www.eso.org/instruments/naco>)

The operation of NAOS and its internal configuration will be largely transparent to the user. This is achieved by the NAOS Preparation Software (PS, [8]). The PS determines the optimal NAOS configuration given external constraints such as brightness of the reference source used for wavefront sensing, angular separation between reference source and science target, or atmospheric conditions. The result of this optimisation is saved in an AO-configuration file (*.aocfg), which in turn is read by the Phase 2 Preparation Software (P2PP). In addition, it provides the user with information on the expected performance taking into account observing conditions. Finally, it delivers to the CONICA ETC the parameters characterising the image peak intensity and the width after AO correction.

Estimates for required exposure times can be obtained from the CONICA exposure time calculator (ETC). The CONICA ETC is closely related to other ETCs for VLT instruments and should thus feel familiar to most users. As a rule of thumb, the overall throughput of NACO is about half that of ISAAC, and required exposure times can be scaled accordingly. Because of the smaller "footprint" of the diffraction-limited Point Spread Function (PSF) of NACO compared to the seeing limited PSF of ISAAC, point source sensitivity in the sky-background limited case tends to be higher for NACO than for ISAAC.

Similar to other VLT instruments, NACO observations are supported by a dedicated set of acquisition, observing and calibration templates. Using P2PP, these templates can be grouped in observing blocks in order to define observing sequences. For each observing block, the AO-configuration file created by the PS has to be specified only once in the corresponding acquisition template.

4.2 Observing with NACO at the VLT

At the time of writing, NACO is still in its commissioning phase, and not all instrument modes have been validated, yet. Initially it is expected to offer imaging and polarimetry from 1 to 4 μm as well as long-slit spectroscopy (R = 500 to 2000) and coronagraphy, though the latter two only with a restricted set of slits and grisms, and coronagraphic masks, respectively. The cryogenic Fabry-Perot and observations in the M-band (still requiring more testing of the chopping mode) will very likely only be offered at a later stage.

A typical observing sequence consists of presetting the telescope to the science target, acquisition of a guide star by the telescope's active optics,

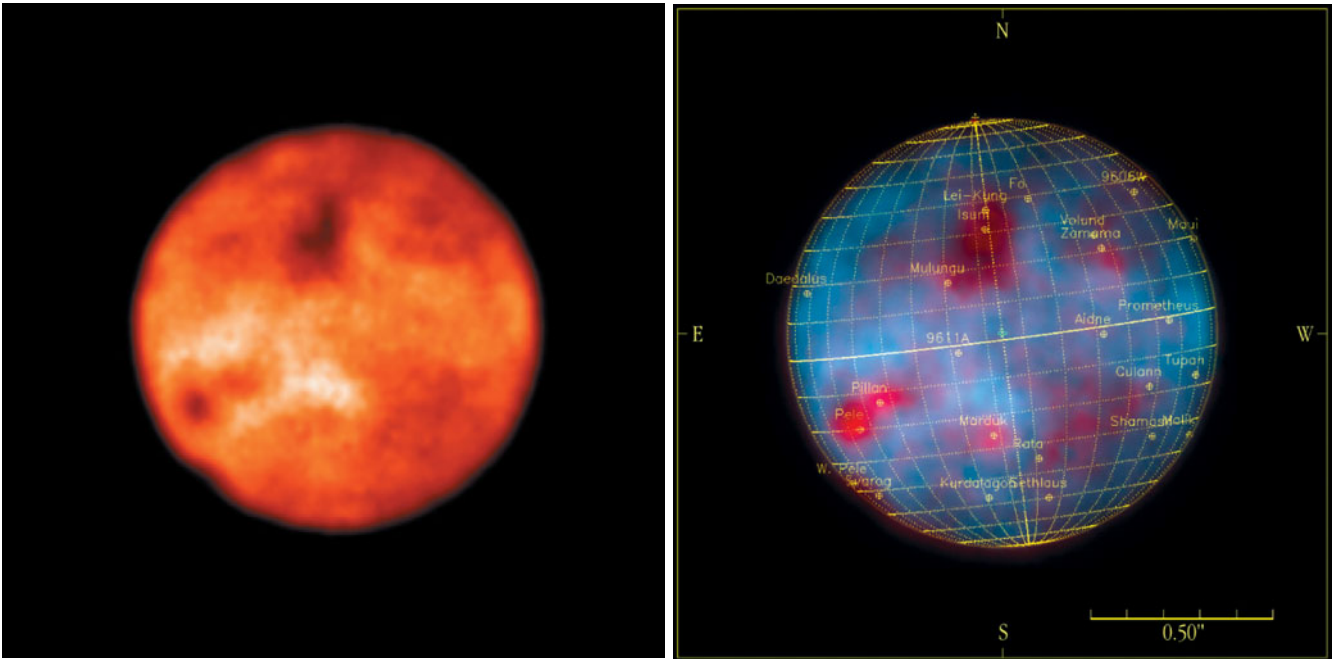


Figure 3: left: Io, the volcanic moon of Jupiter, as imaged with NACO on December 5, 2001, through a near-infrared, narrow-band filter at $2.166 \mu\text{m}$. Despite the small angular diameter of Io of only about $1.2''$, many features are visible at this excellent angular resolution of 60 mas as provided by NACO. Shown on the right is a composite of the same exposure with another obtained at a longer wavelength (L' -filter at $3.8 \mu\text{m}$), with a latitude-longitude grid superposed. Many of the volcanic peaks clearly stand out in the longer-wavelength image.

then the acquisition of the reference source with NAOS, check of exposure times, and finally the start and execution of the observing sequence. Because of the need to acquire a reference source (and to frequently open and close the loop – for instance in the course of dithering or autojitter sequences) instrumental time overheads for NACO tend to be higher than, e.g., for observations with ISAAC. All these steps are, however, handled by the templates and the software controlling NACO, and are hence transparent to the user ([15]).

Calibration data for the most commonly used modes will be obtained on a regular basis by ESO. For more specialised observing modes the individual users are requested to include the calibration needs in the time request.

4.3 Archiving and pipeline

As soon as a NACO data file is saved on the instrument workstation, it is automatically transferred to the archive computer on Paranal. All NACO data will be incorporated in the VLT archive, and be searchable through the database. After the end of the proprietary period, data will become available to astronomers from ESO member countries by access to the VLT archive.

A data pipeline is being developed in order to facilitate quick-look analysis of the data and assessment of the data quality. Pipeline-reduced data will also be distributed together with the raw data files through the VLT archive ([11]). Dedicated software tools will

be made available through the eclipse library ([4]).

5. Initial Results and Science Prospects

While commissioning of NACO is still ongoing, it has been delivering impressive astronomical results virtually from its first hour of operation. Initial results have been publicised in two press releases aimed at providing the ESO community and the general public with a first impression on the unique capabilities of NACO at ESO VLT:

<http://www.eso.org/outreach/press-rel/pr-2001/pr-25-01.html>

<http://www.eso.org/outreach/press-rel/pr-2002/phot-04-02.html>

Science demonstration targets observed include solar-system objects such as Io and Saturn, a nearby free-floating binary brown dwarf, nearby star-forming regions such as the Becklin-Neugebauer object with the associated Kleinmann-Low nebula, T Tauri stars, evolved stars such as Frosty Leo or Eta Car, crowded stellar fields in starburst clusters, and extragalactic objects.

A series of $2.16 \mu\text{m}$ narrow-band images of the prototypical pre-main sequence triple star T Tauri nicely demonstrates the effect of adaptive optics. Shown on the left-hand side of Figure 2 is an open-loop image. The 0.4-sec exposure freezes the speckle pattern, which in a longer exposure will average out to a seeing-limited image with a resolution of $0.5''$. The middle image has been obtained with the AO correction turned on. The right-hand side shows a

K-band spectrum of the two components of T Tauri South.

Io, the innermost of the four Galilean moons of Jupiter and the most volcanically active place in the Solar System was imaged with NACO on December 5, 2001. At the time of observations, Io's diameter of 3660 km corresponded to an angular diameter of $1.2''$. Despite this relatively small diameter, NACO was able to resolve a wealth of details. Many of the volcanic peaks clearly stand out (Fig. 3). With VLT instruments like NACO it will be possible to continue the "volcano watch" on Io from the ground now that the Galileo spaceprobe has expired.

Observations of the Solar System's "Lord of the Rings" were even more challenging than the observations of Io. While CONICA's and hence Yepun's field of view had to be steadied on Saturn, NAOS had to track the small Saturn moon Tethys, which was used as a reference source for wavefront sensing, while the active optics of Yepun had to track a star used for determining active optics corrections and autoguiding. The initial experiment worked very well, and validated the ability of NACO to do off-axis wavefront sensing on "moving targets", while steadying the science beam on a target with different sidereal motion. Observations like these can be used to monitor weather patterns on Saturn, study the fine structure of the rings, and track the movement of smaller moons.

In the morning of February 4, 2002, in the final hour of the 2nd commissioning run, Yepun was pointed to-

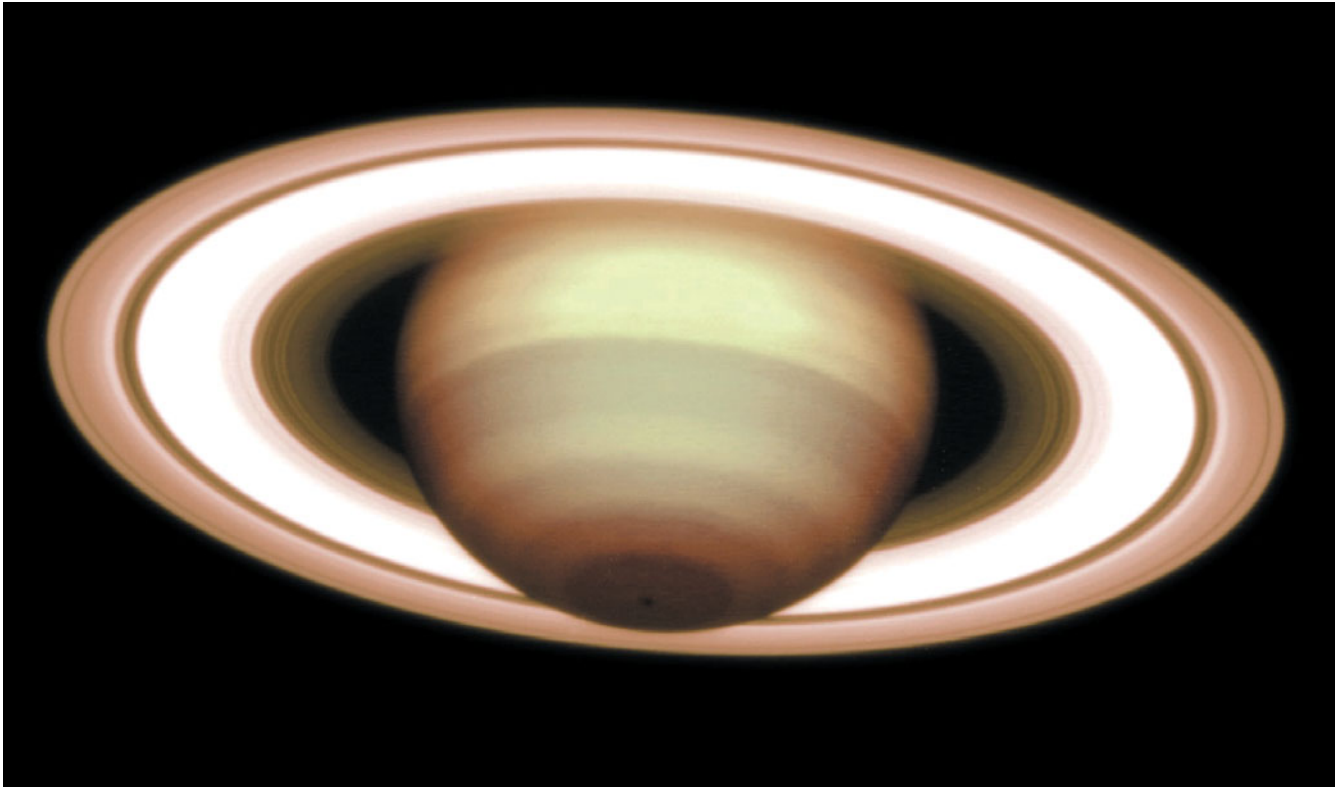


Figure 4: This image shows the giant planet Saturn, as observed with the VLT NAOS-CONICA Adaptive Optics instrument on December 8, 2001. The distance between Earth and Saturn was 1209 million km. It is a composite of exposures in two near-infrared wavebands (H and K) and displays well the intricate, banded structure of the planetary atmosphere and the rings. Note also the dark spot at the south pole at the bottom of the image.

wards the free-floating binary brown dwarf 2MASS1426316+155701 ([3]). Despite atmospheric seeing as determined by the Astronomical Site Monitor at a wavelength of 500 nm varying between 0.8" and 1.2", and an average airmass of 1.4, NAOS was able to

close the loop on the $R = 15.6$ mag ($B-R = 1.0$ mag) binary brown dwarf. Figure 5 shows the closed-loop K-band image (60 sec exposure time), and a 5-min K-band spectrum nicely separating both components of the 0.15" binary. For a distance of 18 pc to

2MASS1426316+155701, 0.15" correspond to a projected separation of 3 AU. Observations like these can be used to monitor the orbital motion of nearby binary brown dwarfs.

Already in the second night of the first commissioning run, NACO closed

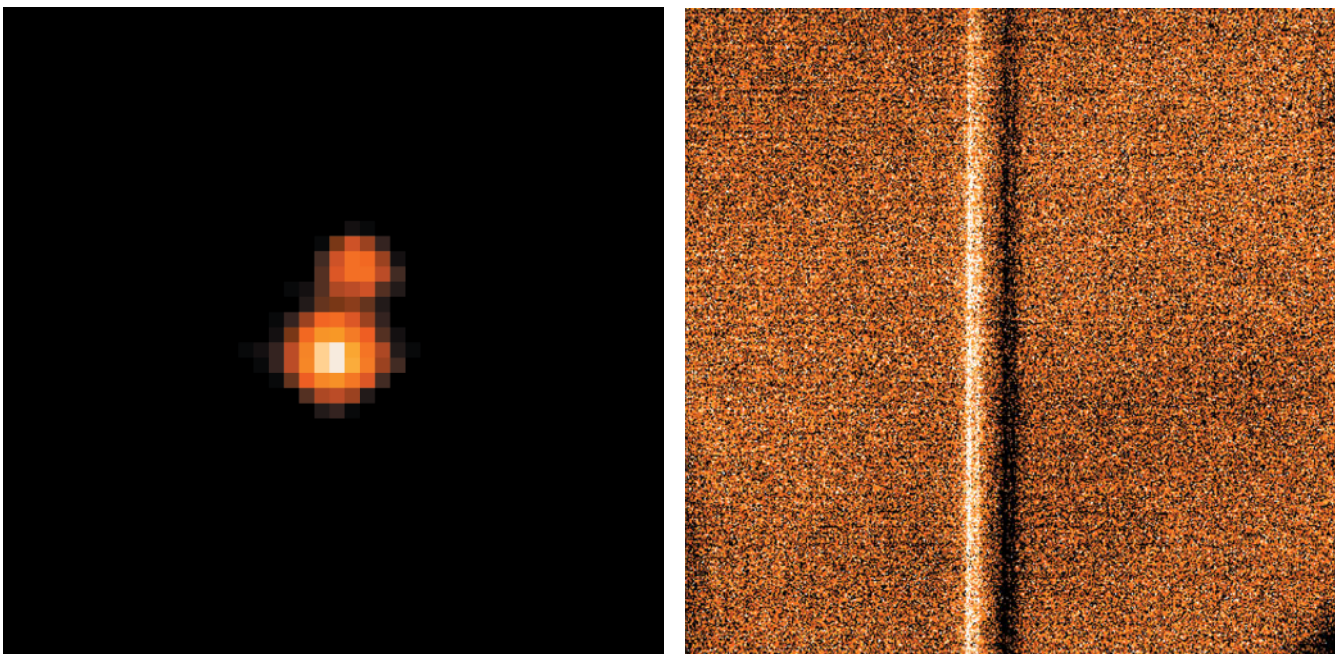


Figure 5: The faint ($R = 15.6$ mag) free floating binary (0.15") brown dwarf 2MASS1426316+155701 nicely resolved by NACO under non-optimal observing conditions. Left: 60-sec K-band image. Right: difference of two 300-sec K-band spectra of the brown dwarf binary. The two binary components with $K = 12.2$ mag and $K = 12.8$ mag are clearly detected.

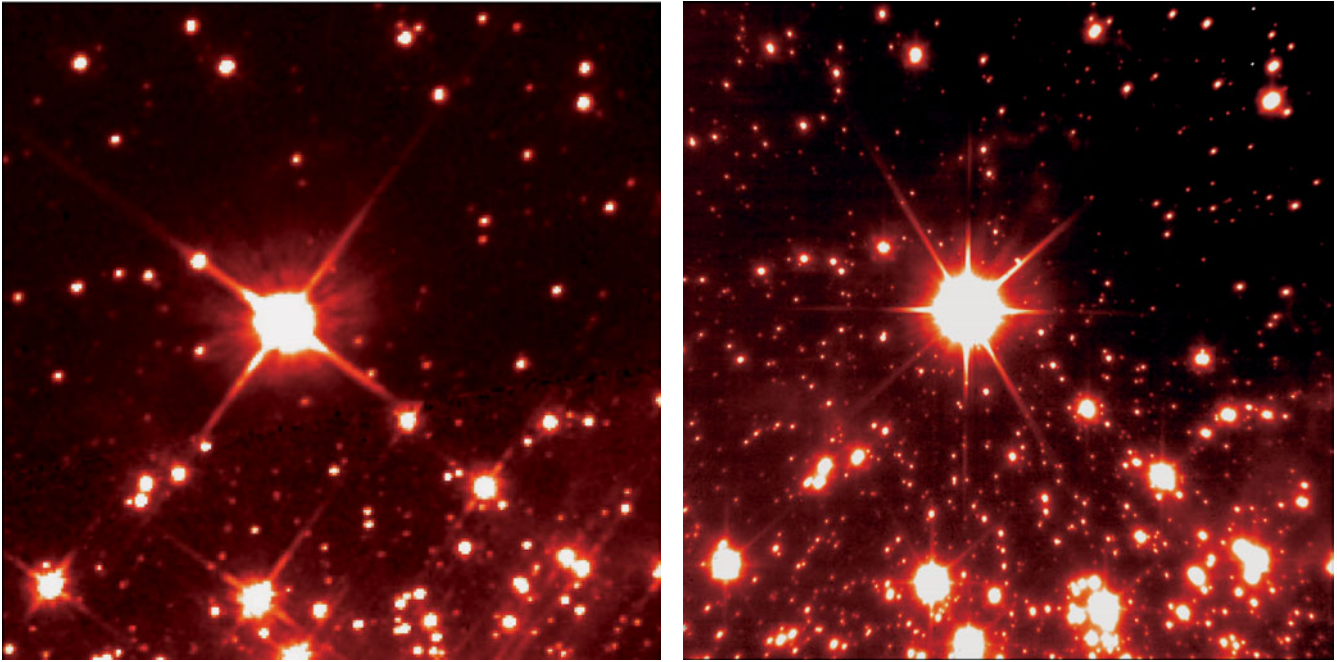


Figure 6: Left: this image of NGC 3603 was obtained with the WFPC2 camera on the Hubble Space Telescope (HST) in the I-band (800 nm). It is a 400-sec exposure and shows the same sky region as in the 300-sec NACO image shown to the right. The image nicely demonstrates that Yepun with NACO is capable of achieving in the K-band the same spatial resolution as HST/WFPC2 at three times shorter observing wavelength of 800 nm (I-band). The HST image was extracted from archival data. HST is operated by NASA and ESA.

the loop on the blue supergiant Sher 25, which is located at a distance of 7 kpc in the NGC 3603 starburst region. A comparison to an HST/WFPC2 image of the same region highlights that – provided a reference source suitable for wavefront sensing is available – NACO at Yepun can achieve in the K-band the same spatial resolution as HST/WFPC2 in the I-band (Figure 6).

6. Outlook: NACO and Beyond

A 3rd (and final) commissioning run of NACO is planned for the period March 22 to April 4, 2002. After this, two runs for instrument “Paranalisation”, and subsequently dry runs (including science verification) are planned before the new VLT instrument is deemed ready for science operations. At the time of writing, it is planned to offer NACO, the 5th VLT instrument to become operational, from Period 70 on to the general ESO community. More details on the proposal process can be found in the Call for Proposals.

In the meantime, work on a panoply of other advanced AO systems for the VLT and VLTI is in progress. The LGS facility at UT4 is expected to come online in 2003. Both NACO and SINFONI (an integral field NIR spectrograph fed by a curvature sensing AO system) will greatly benefit from the increased sky coverage facilitated by a laser guide star. With the implementation of MACAO-VLTI the coude foci of all the four VLT Unit Telescopes at last will also be equipped with AO as was initially envisioned when the original

CONICA proposal was selected more than a decade ago. Adaptive Optics will enable the VLTI to reach still fainter magnitudes, opening a wide range of astronomical objects for research. More details on VLT AO systems and development will be presented in future articles in *The Messenger*.

These projects ensure that the VLT will stay competitive throughout this decade, and give European astronomy a leading edge in studies of the universe.

Acknowledgements: Contributors to the CONICA and NAOS Projects

The NACO project would not have been possible without the dedication of many more people than included in the list of authors of the present article on commissioning activities. An (undoubtedly incomplete) list includes:

- From ONERA: J.M. Conan, L. Rousset-Rouviere, L. Te Toullec.
- From LAO Grenoble: J.-L. Beuzit, G. Chauvin, P. Feautrier, P. Kern, P.-Y. Magnard, P. Rabou, E. Stadler.
- From Observatoire de Paris: R. Arsenault, D. Bauduin, G. Calvet, C. Collin, J. Deleglise, P. Gigan, B. Lefort, M. Lopez, C. Marlot, S. Marteau, G. Michet, J. Montri, G. Nicol, S. Pau, V.D. Phan, B. Talureau, D. Rouan, O. Rondeaux, S. Servan, B. Taureau, P. Van Duoc.
- From MPIA Heidelberg: H. Becker, A. Böhm, P. Granier, W. Laun, K. Meixner, N. Muench, A. Tuscher, K. Wagner.

- From ESO: P. Amico, P. Ballester, J. Beckers, J. Brynnel, C. Cavadore, L. Close, F. Comerón, J.-G. Cuby, C. Cumani, N. Devillard, R. Dorn, G. Finger, M. García, G. Gillet, G. Huster, J. Knudstrup, M. Meyer, M. Peron, A. Prieto, L.P. Rasmussen, D. Silva, J. Stegmaier, M.-H. Ulrich, O. van der Lühe, G. Wiedemann.

References

- [1] Beuzit, J.-L., Brandl, B. et al. 1994, *The Messenger* **75**, 33.
- [2] Bonaccini D., Hackenberg, W. et al. 2001, *The Messenger* **105**, 9.
- [3] Close, L., Potter, D. et al. 2002, *ApJ* **566**, 1095.
- [4] Devillard, N. 1999, *ADASS* **8**, 333.
- [5] Hubin, N., Bertrand, T., Petitjean, P., Delabre, B. 1994a, *SPIE* **2201**, 34.
- [6] Hubin, N., Beuzit, J.-L., Gendron, E., Demailly, L. 1994b, *ICO-16 Satellite Conference on Active and Adaptive Optics*, ed. F. Merkle, p. 71.
- [7] Lenzen, R., Hofmann, R. et al. 1998, *SPIE* **3354**, 606.
- [8] Marteau, S., Gendron, E. et al. 2000 *ADASS* **9**, 365.
- [9] Merkle, F., Hubin, N., Gehring, G., Rigaut, F. 1991, *The Messenger* **65**, 13.
- [10] Meyer, M., Finger, G., Mehrgan, H., Nicolini, G., Stegmaier, J. 1998, *SPIE* **3354**, 134.
- [11] Quinn, P.J., Albrecht, M.A. et al. 1998, *SPIE* **3349**, 2.
- [12] Rabaud et al. 2000 *SPIE* **4007**, 659.
- [13] Rousset, G., Lacombe, F. et al. 2000, *SPIE* **4007**, 72.
- [14] Tessier, E., Bouvier, J., Beuzit, J.-L., Brandner, W. 1994, *The Messenger* **78**, 35.
- [15] Zins, G., Lacombe, F. et al. 2000, *SPIE* **4009**, 395.